JOURNAL OF MATERIALS SCIENCE 31 (1996) 1275–1284

Comparison of the uniaxial tensile modulus and dynamic shear storage modulus of a filled hydroxy-terminated polybutadiene and GAP propellant

E. J. S. DUNCAN, P. BROUSSEAU
Defence Research Establishment Valcartier, Courcelette, Québec, Canada G0A 1R0

The uniaxial tensile moduli for two filled composite solid propellants, one based on a hydroxy-terminated polybutadiene with an ammonium perchlorate oxidizer and the other on a glycidyl azide polymer with a phase-stabilized ammonium nitrate oxidizer, were measured at various temperatures and over a three decade range of strain rates. Dynamic shear moduli were measured at various strains and temperatures over a three decade range of frequencies. Values of the tensile modulus, $E_T/3$ (assuming Poisson's ratio equals 0.5), were compared with the dynamic storage modulus, G', for each of the dynamic strain levels investigated. The results demonstrate that it is possible to compare $3G'$ measured at different dynamic strains and frequencies with the incremental tangent moduli obtained at corresponding uniaxial strains from constant strain rate tests on specimens with a JANNAF geometry. The comparisons are most favourable when the concave-up region of the stress–strain curve extends only up to approximately 2.0% strain. It was observed that G' obtained at a dynamic shear strain of 2.0% provided the best overall correlation with $E_T/3$ measured over a range of temperatures and strain rates.

1. Introduction

Structural and processing demands placed on solid propellants are becoming ever more exacting as their uses become increasingly specialized. This brings about the need for implementing the most advanced characterization techniques possible. To this end, dynamic mechanical spectroscopy has become a widely used methodology for analysing the microstructural and macrostructural character of polymeric systems [1, 2]. It has recently been applied to the characterization of energetic polymers such as propellants [3–6]. Dynamic mechanical analysis offers numerous advantages over conventional tensile mechanical property tests. These include the speed with which tests can be carried out, the reduced amount of material necessary for test specimens and notably, the high degree of sensitivity and reproducibility of the tests. Husband [7] remarked that there is usually clear relationship between the test data and the material's end use performance.

In conventional uniaxial mechanical property testing, a constant rate of deformation is applied to a specimen and the resulting force is measured. The only properties obtainable from the subsequent stress–strain curve are the modulus, maximum stress and strain at maximum stress. These properties, although valuable from the standpoint of failure characteristics, by themselves elucidate little concerning the microstructural/thermal changes known to take place in a polymeric system. The tests provide minimal information on the viscoelastic nature of the material unless many tests are completed at different temperatures and rates of deformation and nothing on the elastic or viscous components that comprise an individual material response.

On the other hand, in dynamic mechanical analysis, a sinusoidal varying strain applied to a linear viscoelastic material will induce a sinusoidal torque (stress) that can be decomposed into an elastic component in phase with the strain and a viscous component 90° out of phase with the strain. The elastic portion is proportional to the dynamic storage modulus, G', and the viscous portion is proportional to the dynamic loss modulus, G''. The ratio of the viscous to elastic component, G''/G', is referred to as the loss tangent, tan δ, and is equal to the tangent of the phase angle between the applied strain and the induced torque. With these basic dynamic properties it is possible to determine key mechanical and thermal transitions relating to the elastic or viscous component, that occur in polymeric materials at both the microstructural level and macrostructural level. Mobility of main chain and major side groups in polymers, and binder/particulate de-wetting in composite polymers, are two examples.

By far most of the mechanical property characterization work on solid propellants has been based on constant strain rate uniaxial tension tests. One reason for this is that structural analysis of solid propellant-based systems require mechanical properties derived from these tests. Within the published domain of dynamic mechanical analysis on loaded polymers, there

0022–2461

is surprisingly little work with a focus on documenting and quantifying the physical relationship between dynamic mechanical properties and conventional uniaxial mechanical properties. While some work is being carried out on the determination of the relaxation spectrum from dynamic mechanical data and vice versa [8–11], it does not specifically address the equivalence of mechanical properties *per se*.

The objective of this study was to compare the dynamic storage modulus measured in shear using rectangular bars and conventional tensile modulus measured in uniaxial tension using JANNAF Class C specimens under a range of dynamic frequencies, constant strain rates and temperatures. The latter are used almost without exception for measuring the conventional mechanical properties of filled polymers. Two filled polymer solid propellants, one based on a hydroxy-terminated polybutadiene with an ammonium perchlorate oxidizer and the other on a glycidyl azide polymer with a phase-stabilized ammonium nitrate oxidizer, were investigated.

2. Theory

Determining the equivalency between the dynamic modulus and the uniaxial tensile modulus necessitates that the moduli be related theoretically and that comparisons be made at "equivalent times" within their respective time domains. It will be instructive to provide a general overview of the theory on which this study is based. The reader is referred to other works [12–14] for a more comprehensive treatment.

2.1. Dynamic shear and uniaxial extension: modulus considerations

In dynamic mechanical spectroscopy analysis, a dynamic shear strain is applied to a specimen, usually rectangular or cylindrical in shape, and the corresponding induced dynamic force (torque) is measured. The dynamic waveform is most often sinusoidal, at a frequency, v, in cycles s^{-1} (Hz) or ω in rad s^{-1} $= (2\pi v)$. The sinusoidal strain is given by

$$\gamma = \gamma^0 \sin \omega t \tag{1}$$

where γ is the shear strain, γ^0 is the maximum amplitude of the strain, ω is the frequency (rad s^{-1}) and t is the time (s). If the material is linear viscoelastic, the stress response will be sinusoidal at the same frequency as the strain, but lagging behind at a phase angle δ

$$\sigma = \sigma^0 \sin(\omega t + \delta) \tag{2}$$

Alternatively, the stress can be expressed in terms of two frequency-dependent functions. This can be derived from the linear viscoelastic constitutive equation for stress in terms of strain

$$\sigma(t) = \int_0^\infty G(t-\tau)\frac{d\gamma(\tau)}{d\tau}d\tau \tag{3}$$

where $\sigma(t)$ is the shear stress as a function of time, $G(t)$ is the relaxation modulus and $\gamma(t)$ is the shear strain as a function of time. Taking the time derivative of Equation 1

$$\dot{\gamma} = \gamma^0 \omega \cos \omega t \tag{4}$$

where the overdot refers to the derivative with respect to time, and substituting Equation 4 into Equation 3 and letting $s = (t - \tau)$, we arrive at

$$\sigma(t) = \int_0^\infty G(s)\gamma^0 \omega \cos[\omega(t-s)]\,ds \tag{5}$$

or from trigonometric relations

$$\sigma(t) = \gamma^0\left[\omega\int_0^\infty G(s)\sin \omega s\,ds\right]\sin \omega t + \gamma^0\left[\omega\int_0^\infty G(s)\cos \omega s\,ds\right]\cos \omega t \tag{6}$$

The quantities between the square brackets in Equation 6 are defined as the shear storage modulus, G', and the shear loss modulus, G'', where

$$G' = \omega\int_0^\infty G(s)\sin \omega s\,ds \tag{7}$$

$$G'' = \omega\int_0^\infty G(s)\cos \omega s\,ds \tag{8}$$

G' is directly proportional to the average amount of energy stored and recovered per cycle (elastic energy), while G'' is directly proportional to the average amount of energy lost through various viscous dissipative processes per cycle.

For a perfectly elastic solid, or a viscoelastic solid at equilibrium, the shear modulus, G, is related to the uniaxial tensile modulus, $E_T = \sigma_T/\varepsilon$ (where σ_T is the uniaxial tensile stress and ε is the uniaxial strain) through the relationship

$$G = \frac{E_T}{2(1+\nu)} \tag{9}$$

where ν is the Poisson's ratio. In certain polymeric materials, ν may approach 0.5 (e.g. 0.499) and remain effectively constant over a range of time scales. Under these conditions the relationship expressed by Equation 9 reduces to

$$G = \frac{E_T}{3} \tag{10}$$

which implies that simple shear is directly related to simple uniaxial extension by a factor of 1/3. In physical terms, this occurs because the change in volume during deformation is imperceptible relative to the change in shape. It follows that G' should also be related to E_T in the manner of Equation 10, assuming negligible changes in volume.

2.2. Constant strain rate and dynamic frequency considerations

Correlating G' and E_T, when E_T is dependent on strain rate and G' is dependent on frequency, necessitates

that values be compared at equivalent measures of strain rate and frequency. In the experimental work presented here, G' was measured in shear under a variable rate of shear-strain, $\dot{\gamma}$, while E_T was measured in uniaxial tension under a constant uniaxial strain rate, $\dot{\varepsilon}$. In a practical sense, $\dot{\varepsilon}$ refers to the rate of change with time of the extension of an infinitesimal element of material in the direction of loading, while $\dot{\gamma}$ refers to the rate of change with time of the change in the angle formed by two faces of an infinitesimal element of material in the plane of loading. For the purposes of this paper $\dot{\gamma}$ and $\dot{\varepsilon}$ are defined in the following way

$$\dot{\varepsilon} = \dot{\varepsilon}_{11} = \frac{\partial}{\partial x_1}\left(\frac{\partial u_1}{\partial t}\right) \quad (11)$$

and

$$\dot{\gamma} = \dot{\gamma}_{12} = \frac{\partial}{\partial x_1}\left(\frac{\partial u_2}{\partial t}\right) + \frac{\partial}{\partial x_2}\left(\frac{\partial u_1}{\partial t}\right) \quad (12)$$

where δx_1 and δx_2 are the incremental lengths along the x_1 and x_2 coordinate axes respectively and δu_1 and δu_2 are the incremental displacements in each coordinate direction.

A relationship has been derived that relates frequency used in dynamic tests to an average (constant) strain rate. The time derivative of Equation 1 is

$$\dot{\gamma} = \gamma^0 \omega \cos \omega t \quad (13)$$

To find the average strain rate, $\bar{\dot{\gamma}}$, over the interval from 0 to $\pi/2\omega$ where $\gamma = \gamma^0$, Equation 13 is integrated and divided by the interval $\pi/2\omega$

$$\bar{\dot{\gamma}} = \left(\frac{\pi}{2\omega}\right)^{-1} \int_0^{\pi/2\omega} \gamma^0 \omega \cos \omega t \, dt \quad (14)$$

the answer to which is

$$\bar{\dot{\gamma}} = \frac{2\omega\gamma^0}{\pi} \quad (15)$$

To obtain an average strain rate in uniaxial tension which is equivalent to $\bar{\dot{\gamma}}$ for a given ω and γ_0 from a dynamic test, Equation 15 is rewritten as

$$\dot{\varepsilon} = \frac{2\omega\gamma^0}{\pi} \quad (16)$$

where $\dot{\varepsilon}$ is the uniaxial constant strain rate (s^{-1}), ω is the frequency (rad s^{-1}) and γ^0 is the maximum amplitude of the strain at the given ω. Rewriting as ω in terms of $\dot{\varepsilon}$ we have

$$\omega = \frac{\dot{\varepsilon}\pi}{2\gamma^0} \quad (17)$$

3. Experimental procedure

Two filled solid propellants were investigated in this study. One is based on a conventional inert polymer binder composed of a urethane cross-linked hydroxy-terminated polybutadiene (HTPB) polymer into which is dispersed particulate ammonium perchlorate (AP) as the oxidizer. The other is based on an energetic polymer binder known as glycidyl azide polymer (GAP) into which is dispersed particulate phase-stabilized ammonium nitrate (PSAN) as the oxidizer. The solids loading is 88% by weight for the HPTB/AP propellant and 71% by weight for the GAP/PSAN propellant.

Constant strain rate uniaxial tensile mechanical properties of two propellants, GAP/PSAN and HTPB/AP, were measured over three decades of strain rate (0.000 0967–0.0967 s^{-1}) and at five different temperatures (− 40, − 30, 0, 20 and 60 °C) for the GAP/PSAN and (− 65, − 30, 0, 23 and 60 °C) for the HTPB/AP. Three specimens were tested at each strain rate and temperature. Standard JANNAF [15] "dog-bone" test specimens were used. Each specimen was die-cut from a pre-cast 12.7 mm thick slab. The effective gauge length for the geometry of the specimens was determined using a laser extensometer and found to be 86.5 mm at a strain rate of 0.009 67 s^{-1} and room temperature. The effective gauge length is the length which divided into the displacement of the crosshead gives a number equal to the strain in the centre of the test specimen. This value was used for all tests. The strain was calculated by dividing the change in the displacement by the effective gauge length. Testing was completed on an Instron Model 1122 with a temperature box and controller. All specimens were preconditioned at the test temperature for approximately 1 h prior to testing.

Instron Series IX software was used for data acquisition and data reduction. The tensile modulus for materials that characteristically respond with a low stress, concave-up region during the early stages of a test, such as filled composite propellants, was determined by computing a "least squares fit" straight line through consecutive segments of data, beginning at the start of the test and progressing along the curve up to the maximum stress. The highest slope measured was defined as the tensile modulus.

Dynamic mechanical properties G', G'' and G^* were mesaured using a Rheometrics Dynamic Mechanical Spectrometer model II (RDS-II). Tests, referred to as dynamic frequency/temperature sweeps, were completed in dynamic shear over a three decade range of frequency (0.1–100 rad s^{-1}) between temperatures of − 40 and 55 °C for GAP/PSAN and − 70 and 80 °C for HTPB/AP. A 15 °C temperature step with a 10 min soak interval between each, was used in both series. Seven different strain levels (0.1%, 0.5%, 1.0%, 2.0%, 3.0%, 4.0% and 5.0%) were investigated for GAP/PSAN and six strain levels (0.1%, 0.5%, 1.0%, 2.0%, 3.0% and 4.0%) were investigated for HTPB/AP. Specimens were die-cut from pre-cast 12.7 mm thick slabs and were rectangular in form with a test-size dimension of approximately 48.8 mm × 12.7 mm × 4.1 mm.

Rheometrics Rhecalc software was used for all time–temperature superposition analyses on the dynamic frequency/temperature data as well as the constant strain rate data.

4. Results and discussion

It has long been recognized that loading rate and temperature have a direct influence on mechanical properties such as modulus, strength and strain capability of filled polymer solid propellants. Considering

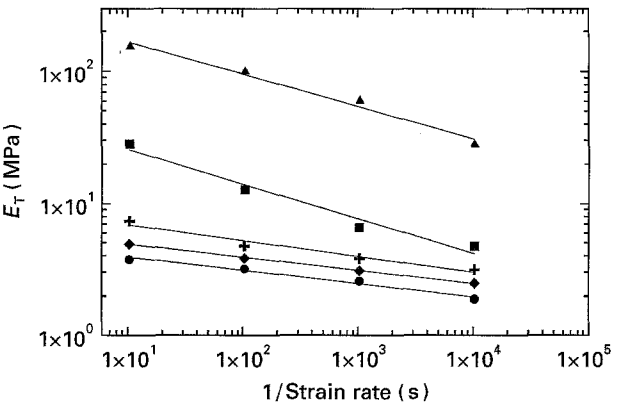

Figure 1 Tensile modulus, E_T, from uniaxial constant strain rate tests on HTPB/AP at (▲) − 65 °C, (■) − 30 °C, (+) 0 °C, (◆) 23 °C and (●) 60 °C and over a three decade range of strain rates.

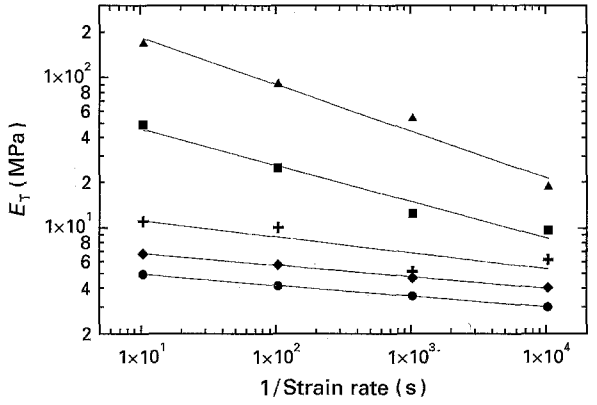

Figure 2 Tensile modulus, E_T, from uniaxial constant strain rate tests on GAP/PSAN at five different temperatures (▲) − 40 °C, (■) − 30 °C, (+) 0 °C, (◆) 23 °C and (●) 60 °C and over a three decade range of strain rates (from [16]).

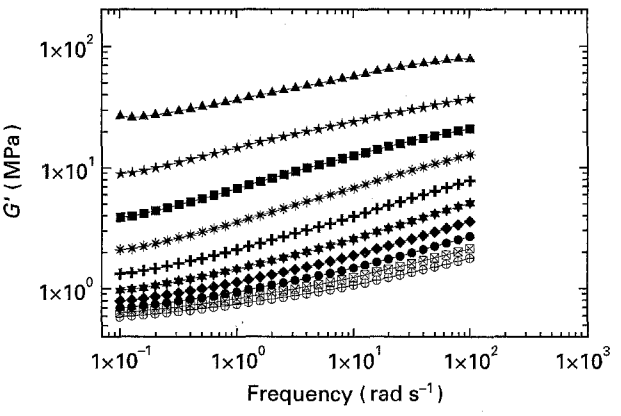

Figure 3 Dynamic storage modulus, G', from a frequency/ temperature sweep test on HTPB/AP at 2.0% strain, ten different temperatures and over a three decade range of frequency. (▲) − 67 °C, (★) − 52 °C, (■) − 37 °C, (×) − 22 °C, (+) − 7 °C, (✱) 8 °C, (◆) 23 °C, (●) 38 °C, (⊠) 53 °C, (⊕) 68 °C.

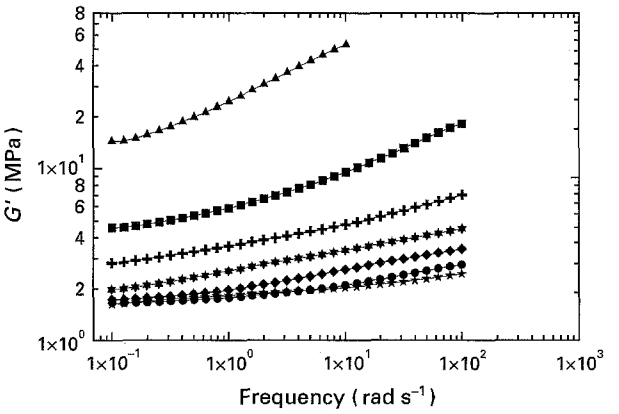

Figure 4 Dynamic storage modulus, G', from a frequency/ temperature sweep test on GAP/PSAN at 2.0% strain, seven different temperatures and over a three decade range of frequency. (▲) − 37 °C, (■) − 22 °C, (+) − 7 °C, (✱) 8 °C, (◆) 23 °C, (●) 38 °C, (★) 53 °C.

the viscoelastic nature of filled polymers, any valid comparison of dynamic moduli with conventional uniaxial moduli necessitates that they be compared at equivalent rates of loading. Such a relation is given by Equation 17, which calculates the dynamic frequency that corresponds to a given constant strain rate at a specified level of dynamic strain. The G' associated with this frequency may be compared to the maximum tangent modulus if certain assumptions are made: (i) the average shear strain rate $\bar{\dot{\gamma}}$ is proportionally equivalent to a constant uniaxial strain rate, $\dot{\varepsilon}$, as implied by equations 15 and 16, and (ii) Poisson's ratio equals 0.5 (Equations 9 and 10).

The effect of $\dot{\varepsilon}$ and temperature on the tensile modulus, E_T, of HTPB/AP is illustrated in Fig. 1. Each data point represents the average of three tests at the same nominally constant strain rate. Two features are evident from the data presented in Fig. 1. The first is the log-linearity of the data across three decades of strain rate at all temperatures. Second, there is a progressive increase in the slope of the curves between 23 and − 30 °C. Above 23 °C and below − 30 °C the slope of the curves remains at a relatively constant value. Similar trends have been observed for GAP/PSAN propellant (Fig. 2) [16].

The dynamic equivalent to a series of conventional uniaxial tests at different strain rates and temperatures is a dynamic frequency/temperature sweep analysis. In this test a specimen is subjected to a sinusoidal varying strain over a range of frequencies and at various temperatures. Typical results for G' from a frequency/temperature sweep on HTPB/AP and GAP/PSAN at a strain of 2%, are presented in Figs 3 and 4, respectively. The trends exhibited under a sinusoidal displacement regime are generally consistent with those obtained from the constant uniaxial strain rate tests. The moduli are observed to increase with increasing rate of frequency or rate of strain and decreasing temperature (note that the reciprocal of strain rate is shown in Figs 1 and 2, which accounts for the negative rather than positive slope). Frequency/ temperature sweeps at progressively higher strains gave rise to systematically lower values of the dynamic moduli for both filled polymer solid propellants tested. This is illustrated in Fig. 5 for the storage modulus, G', obtained from sweeps at five different strain levels, 0.1%, 0.5%, 2.0%, 4.0% and 5.0%, on GAP/PSAN at 23 °C. Non-linear behaviour of this

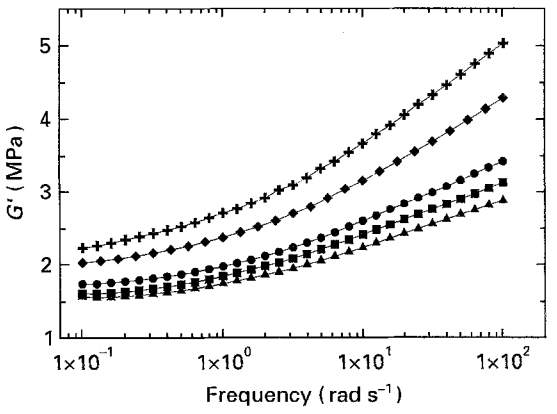

Figure 5 Frequency sweep at five different strain levels on GAP/SPAN at 23 °C. (+) 0.1%, (◆) 0.5%, (●) 2.0%, (■) 4.0%, (▲) 5.0%.

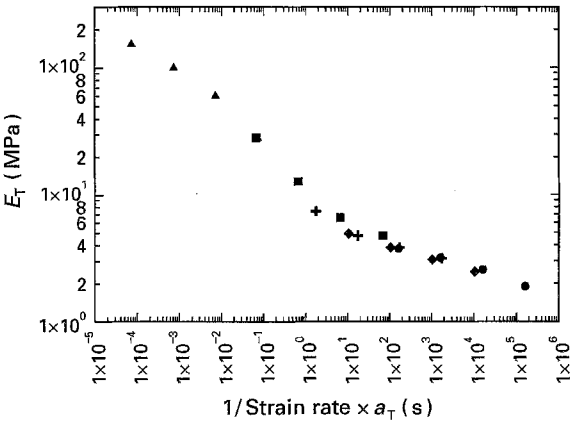

Figure 6 Shifted master E_T curve for HTPB/AP uniaxial constant strain rate data. The reference temperature is 23 °C. (▲) − 65 °C, (■) − 30 °C, (+) 0 °C, (◆) 23 °C, (●) 60 °C.

type in similar highly filled elastomers has been observed by others [1, 2] and is associated with complex filler–filler and filler–binder interactions.

Shifted master G' curves for both the conventional uniaxial test results (Figs 6 and 7) and the dynamic test results (Figs 8 and 9) were constructed using the Williams, Landel and Ferry (WLF) equation

$$\log a_T = \frac{-C_1(T - T_r)}{(C_2 + T - T_r)} \quad (18)$$

where a_T is the shift factor, C_1 and C_2 are constants, T is the temperature and T_r is the reference temperature. Ferry provides a detailed theoretical discussion of time–temperature superposition [12]. The G'' master curves that are shown along side the G' curves in Figs 8 and 9 were constructed using the shift factors determined from the G' data. Note the poor superposition of GAP/PSAN G'' data in the higher shifted frequency region (the undulating nature of the solid line data curve marks its trace through individual data points in the overlapping region of the shifted data). This was observed at all strains and contrasts markedly with the G'' results for HTPB/AP, which superposed very favourably with the shift factors derived from G' data. Stacer and Husband [2] observed a similarly poor superposition for filled GAP in the lower frequency region and suggested that it may reflect a more thermorheologically complex behaviour.

While the use of the WLF equation for thermorheologically complex materials may not be correct in the strictest sense, it is used here to illustrate the degree of commonality between the shift coefficients obtained from constant strain rate tests and dynamic tests at different levels of strain. The WLF equation, constants C_1 and C_2 were calculated using the RDS-II Rhecalc software package and are given in Tables I and II. Although the constants obtained for the HTPB/AP constant strain rate tests appear to be somewhat higher, particularly C_2, than those determined from the dynamic tests at the various levels of strain (Table I), plotting a_T versus the corrected temperature $T - T_r$ (Fig. 10a), shows that the results from both test methodologies are, in general, very consistent at $T - T_r$ values above − 20 °C. At lower values the variability increases, approaching two

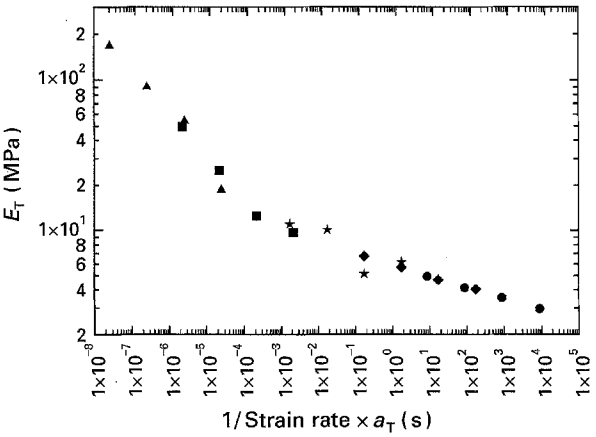

Figure 7 Shifted master E_T curve for GAP/PSAN uniaxial constant strain rate data. The reference temperature is 23 °C. (▲) − 40 °C, (■) − 30 °C, (★) 0 °C, (◆) 23 °C, (●) 60 °C.

decades at − 90 °C. A comparison of the GAP/PSAN WLF constants (Table II) shows, ignoring the dynamic test results at 1% strain where the application of temperature went from hot to cold rather than from cold to hot, that the C_1 and C_2 values are similar for both the constant strain rate and dynamic tests. The values of a_T for the constant strain rate data were determined by manually shifting the data. Fig. 10b shows the results of a_T versus the corrected temperature $T - T_r$ at the various levels of strain. The variability within the GAP/PSAN results is similar to that observed for the HTPB/AP at the lower corrected temperatures and more prevalent, up to one decade, at corrected temperatures above 0 °C.

When comparing G' and E_T it becomes important to consider the form of the stress–strain response, particularly that derived from a specimen with a JANNAF geometry. The authors have observed that for most filled polymer solid propellants, a JANNAF geometry will give rise to a stress–strain curve characteristized by an initial concave-up region. The strain interval over which the upward concavity extends is related both to the temperature and the rate of loading experienced by the specimen. An example of this is shown for GAP/PSAN at 23 °C and a strain

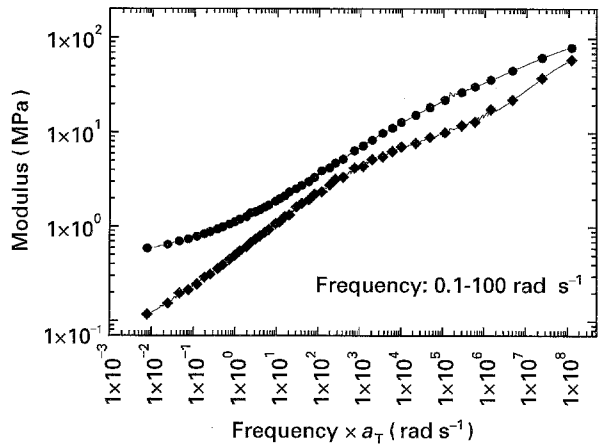

Figure 8 Shifted master (●) G' and (◆) G'' curve for HTPB/AP at 2.0% strain. The reference temperature is 23 °C.

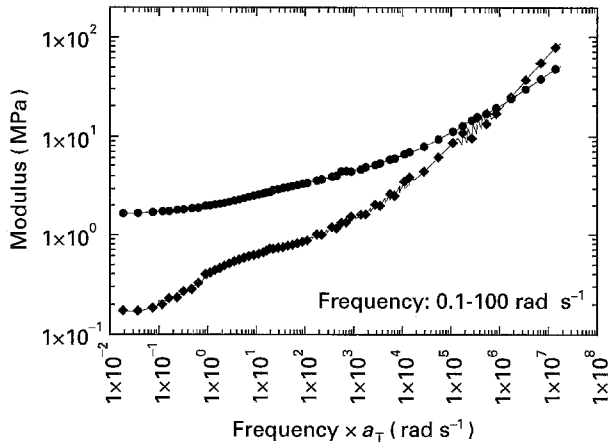

Figure 9 Shifted master, (●) G' and (◆) G'' curve for GAP/PSAN at 2.0% strain. The reference temperature is 23 °C.

TABLE I The WLF equation constants C_1 and C_2 for HTPB/AP propellant

Test type		C_1	C_2
Constant strain rate		7.1	213
Dynamic freq./temp.	0.1%	6.0	166
	0.5%	6.2	186
	1.0%	5.4	160
	2.0%	5.1	163
	3.0%	4.9	157
	4.0%	4.7	154

TABLE II The WLF equation constants C_1 and C_2 for GAP/PSAN propellant

Test type		C_1	C_2
Constant strain rate		8.2	134
Dynamic freq./temp.	0.1%	7.3	117
	0.5%	7.2	126
	1.0%	12.0	153
	2.0%	7.0	128
	3.0%	5.7	112
	4.0%	7.3	126

rate of 0.009 67 s^{-1} in Fig. 11a. In general, at higher temperatures and lower strain rates the concave-up region extended over a larger strain interval. For example, it was determined that the interval at 23 °C

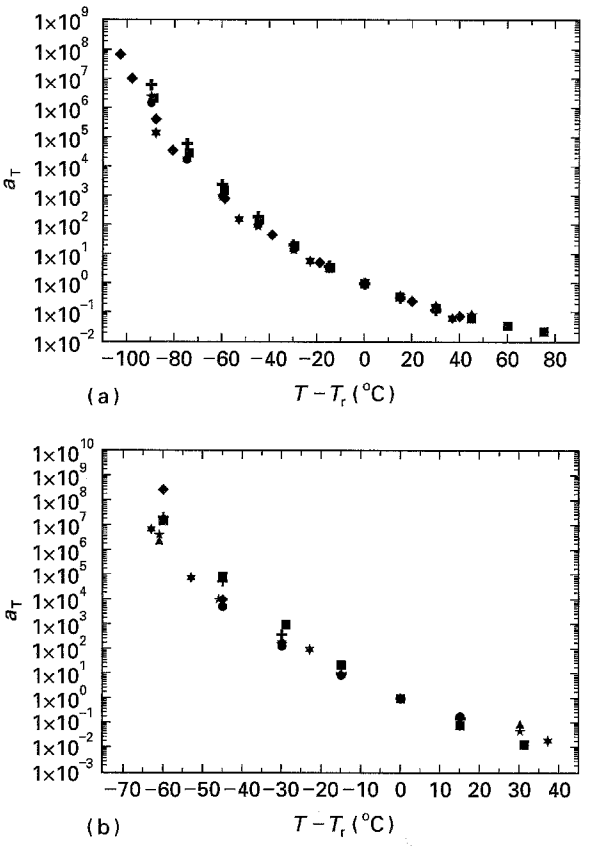

Figure 10 Comparison of the (a) HPTB/AP and (b) GAP/PSAN shift factors, determined from the series of (★) constant strain rate tests and those obtained from the frequency/temperature sweeps at different strain levels: (★) (a) 23 °C, (b) 24 °C; (+) 23%, 0.1%; (◆) (a) 24 °C, (b) 23 °C, 0.5%; (■) (a) 20 °C, (b) 24 °C, 1.0%; (●) 23 °C, 2.0%; (▲) 23 °C, 3.0% (★) 23 °C, 4.0%.

and 0.009 67 s^{-1} was in excess of four times greater than the interval at − 40 °C and 0.0967 s^{-1}. For obvious reasons, a representative uniaxial tensile modulus cannot be obtained from this initially concave-up region of the stress–strain curve. The tensile modulus has been defined for the purposes of this study as the incremental tangent modulus with the highest value and is calculated by means of a moving point linear regression along the stress–strain curve. The strain that develops over the concave-up portion of the stress–strain curve up to the inflection point where the maximum tangent modulus occurs, is assumed not to be representative of the true strain and is replaced by a curve with the slope of the maximum tangent modulus. The offset strain, equal to the strain where the maximum tangent modulus intersects the strain axis, is subtracted to zero the strain. The result is a stress–"adjusted strain" curve. Fig. 11b shows the stress–"adjusted strain" curve for the GAP/PSAN stress–strain data presented above.

Applying Equations 10 and 17, values of $3G'$ obtained from the dynamic frequency/temperature sweep results at each level of strain are presented together with the incremental tangent moduli calculated from three different stress–"adjusted strain" data sets (Figs. 12–14). Two of these are for GAP/PSAN; the first at 23 °C and a strain rate of 0.009 67 s^{-1} and the second at − 40 ° C and a strain

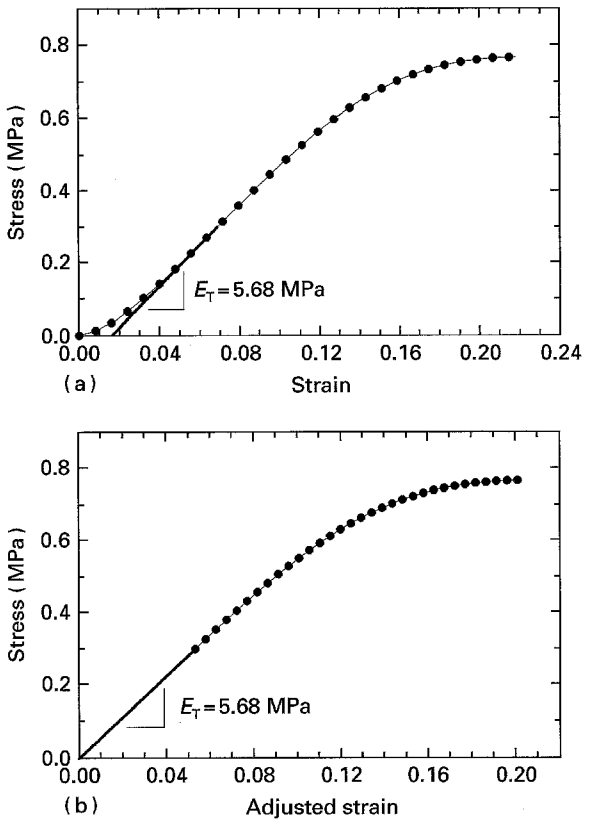

Figure 11 (a) Stress–strain curve obtained from a GAP/PSAN JANNAF specimen tested at a constant strain rate of 0.00967 s^{-1} and 23 °C; (b) stress–"adjusted strain" curve derived from above results. The thick solid line is the maximum tangent modulus (uniaxial tensile modulus).

rate of 0.0967 s^{-1}. The third is for HTPB/AP at − 65 °C and a strain rate of 0.0967 s^{-1}.

The temperature at which the value of G' were considered were the same or within 2–3 °C of those for the uniaxial data. Limitations in the acquisition of the dynamic data meant that it was not possible to obtain a value of G' at a frequency measured experimentally that corresponded exactly to the frequency calculated from Equation 17. Observed differences were generally less that 10%. Table III provides the calculated values of ω from Equation 17 for various constant uniaxial strain rates and maximum dynamic shear strain levels. Not surprisingly, values of $3G'$ at the lowest dynamic strains were higher than the maximum uniaxial tangent moduli determined at similar levels of strain from the JANNAF specimen geometry (Fig. 12). This is true even at very fast loading rates and low temperatures approaching the glass transition temperature (Figs 13 and 14), where the concave-up portion is less extensive. The glass transition temperature of GAP/PSAN was determined to be -40 ± 1 °C and for HTPB/AP, -82 ± 1 °C. At low temperatures and frequencies corresponding to the highest strain rates, values of $3G'$ showed the same general trend as the incremental tangent moduli, decreasing with increasing strain, although always at a lower rate. Values of $3G'$ were as much as 30% higher than the incremental tangent moduli at 5.0% strain for GAP/PSAN and 60% higher for HTPB/AP at 3.0% strain. The latter is due to the fact that HTPB/AP has a uniaxial strain capacity

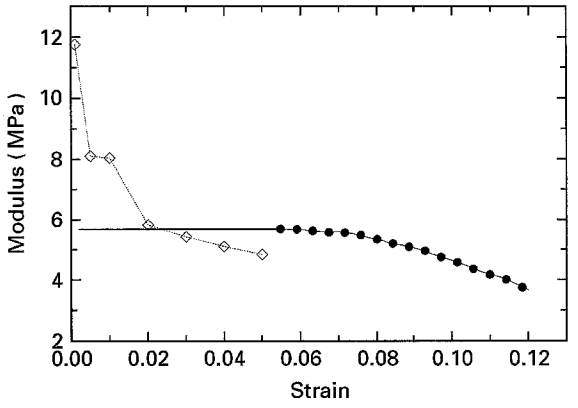

Figure 12 Aplication of equations 10 and 17 to compare (◇) $3G'$ obtained from dynamic frequency/temperature sweeps at seven different levels of strain with (●) the incremental tangent moduli calculated from the stress–"adjusted strain" results of GAP/PSAN shown in Fig. 11b. The thick solid line is the maximum tangent modulus.

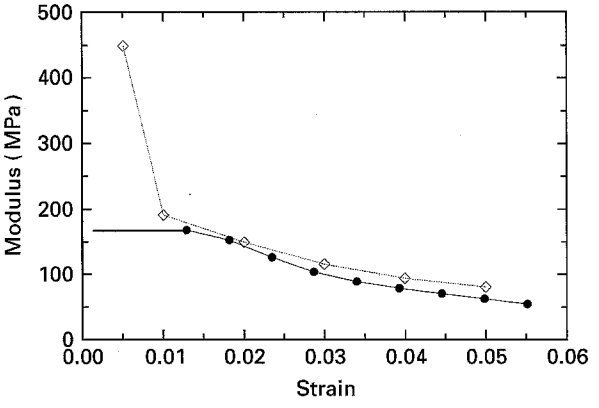

Figure 13 Application of equations 10 and 17 to compare (◇) $3G'$ obtained from dynamic frequency/temperature sweeps at six different levels of strain with (●) the incremental tangent moduli calculated from the stress–"adjusted strain" results of GAP/PSAN at − 40 °C and a constant strain rate of 0.0967 s^{-1}. The thick solid line is the maximum tangent modulus.

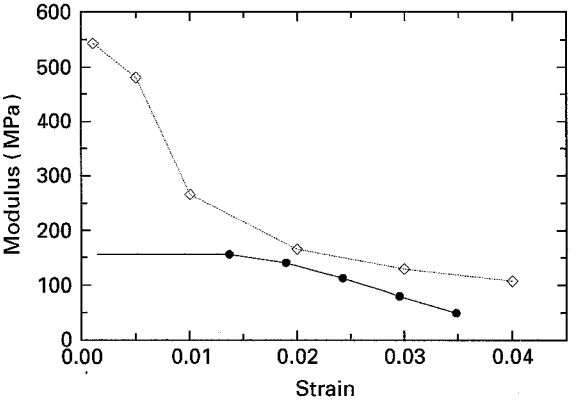

Figure 14 Application of equations 10 and 17 to compare (◇) $3G'$ obtained from dynamic frequency/temperature sweeps at six different levels of strain with (●) the incremental tangent moduli calculated from the stress–"adjusted strain" results of HTPB/AP at − 65 °C and a constant strain rate of 0.0967 s^{-1}. The thick solid line is the maximum tangent modulus.

of only 5.0% at this low temperature and high strain rate (approximately half that of GAP/PSAN), consequently the difference between $3G'$ and the incremental tangent moduli becomes very large as the strain at

TABLE III Values of ω calculated from equation 23 at the strain rates shown

Peak dynamic strain, γ°	ω (rad s^{-1})		
	0.000967 s^{-1}	0.00967 s^{-1}	0.0967 s^{-1}
0.1	1.52	15.2	151.9
0.5	0.304	3.04	30.4
1.0	0.152	1.52	15.2
2.0	0.076	0.759	7.59
3.0	0.051	0.506	5.06
4.0	0.038	0.380	3.80
5.0	0.030	0.304	3.04

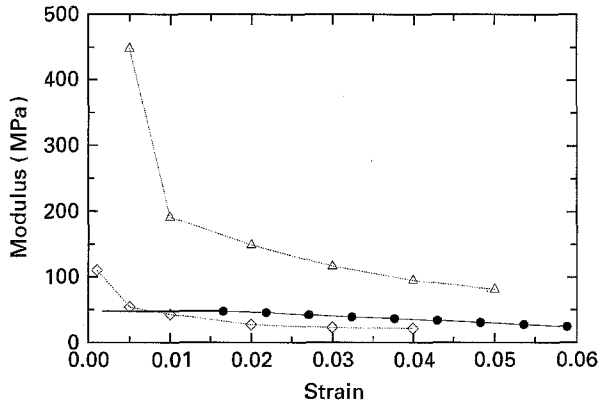

Figure 15 Application of equations 10 and 17 to compare (△, ◇) $3G'$ obtained from dynamic frequency/temperature sweeps on GAP/PSAN at different levels of strain and at (△) − 36 °C, and (◇) − 22 °C, with (●) the incremental tangent moduli calculated from the stress–"adjusted strain" results at − 30 °C. The thick solid line is the maximum tangent modulus.

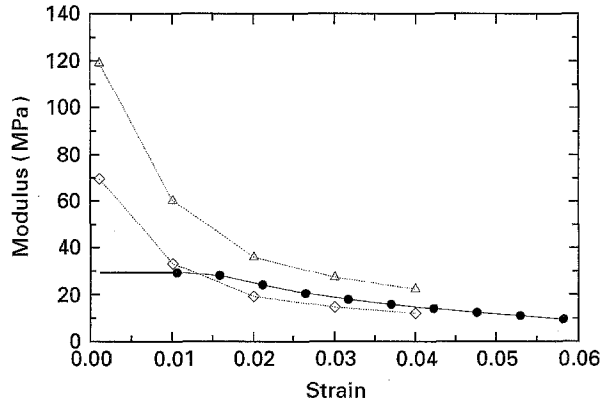

Figure 16 Application of equations 10 to 17 to compare (△, ◇) $3G'$ obtained from dynamic frequency/temperature sweeps on HTPB/AP at different levels of strain and at (△) − 36 °C, and (◇) − 22 °C, with (●) the incremental tangent moduli calculated from the stress–"adjusted strain" results at − 30 °C. The thick solid line is the maximum tangent modulus.

maximum stress is attained. The results shown in Fig. 14 suggest that the maximum strain capacity in shear is higher than the maximum uniaxial strain capacity at equivalent temperatures and rates of loading.

As Figs 15 and 16 illustrate, the relationship between the incremental moduli and $3G'$ remains consistent at higher temperatures at similarly high rates of strain (0.0967 s^{-1}). In both instances the uniaxial

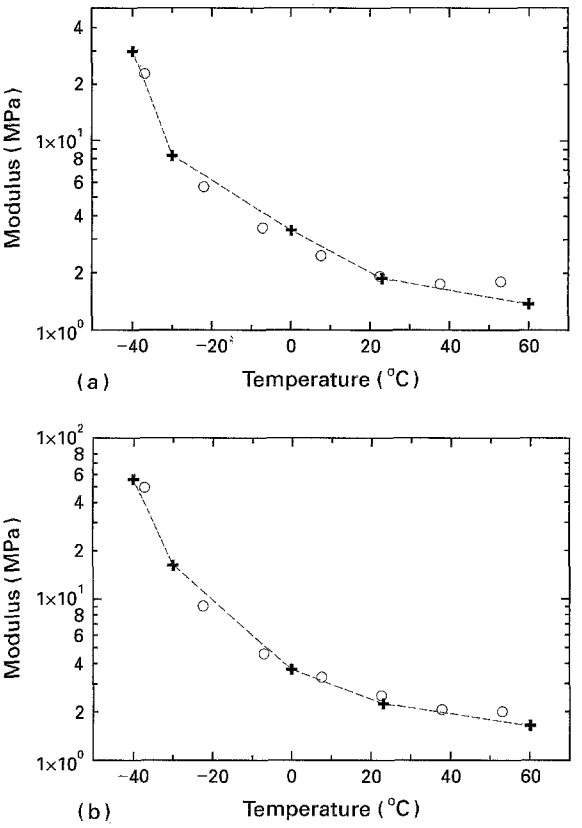

Figure 17 Comparison of GAP/PSAN moduli $E_T/3$ (+) at a strain rate of (a) $\dot{\varepsilon} = 0.00967$ s^{-1} and (b) $\dot{\varepsilon} = 0.0967$ s^{-1} with (○) G' values measured at a dynamic strain of 2% and a frequency of (a) 0.79 rad s^{-1} and (b) 7.9 rad s^{-1}. The theoretical equivalent frequencies calculated from Equation 17 are (a) 0.76 rad s^{-1} and (b) 7.6 rad s^{-1}.

results at − 30 °C fall between the dynamic results at − 22 and − 36 °C. The larger difference between the GAP/PSAN uniaxial data and the − 36 °C dynamic results is related to the closeness of the dynamic data to the T_g of GAP/PSAN at − 40 °C. At higher temperatures and frequencies corresponding to lower strain rates (Fig. 12), values of $3G'$ were often lower than the incremental tangent moduli but their trend suggests that they may approach values of the incremental tangent moduli at higher levels of strain.

It was noted that, in general, over the range of temperatures and rates of loading considered in this study, those values of $3G'$ obtained at a dynamic strain of 2% were consistently found to be the closest to values of E_T when the comparisons are made at similar temperatures and rates of loading. The reason that the equivalency is found at 2.0% strain would seem to be related to the opposing forms of the modulus response, which decreases continuously with increasing strain for the dynamic tests and initially increases with increasing strain over the concave-up portion of the stress–strain curve for the conventional uniaxial constant strain rate tests. Changing the assumptions given earlier would result in the equivalency occurring at a different level of strain. However, in applying Equation 17, the trends are reproducible over a range of temperatures and at different decades of strain for both GAP/PSAN and HTPB/AP propellants. Examples of these results are presented in

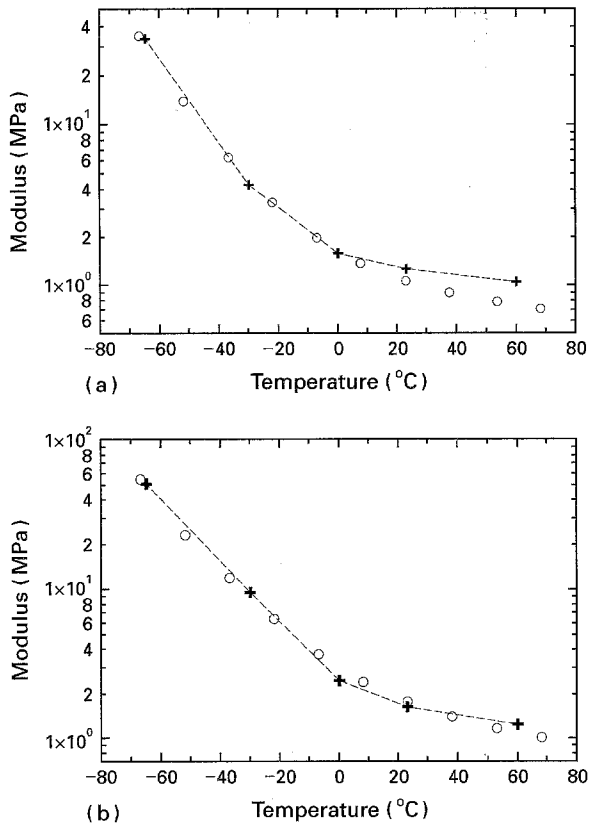

Figure 18 Comparison of HTPB/AP moduli $E_T/3$ (+) at a strain rate of (a) $\dot{\varepsilon} = 0.00967\ s^{-1}$ and (b) $\dot{\varepsilon} = 0.0967\ s^{-1}$ with (○) G' values measured at a dynamic strain of 2% and a frequency of (a) 0.79 rad s^{-1} and (b) 7.9 rad s^{-1}. The theoretical equivalent frequencies calculated from Equation 17 are (a) 0.76 rad s^{-1} and (b) 7.6 rad s^{-1}.

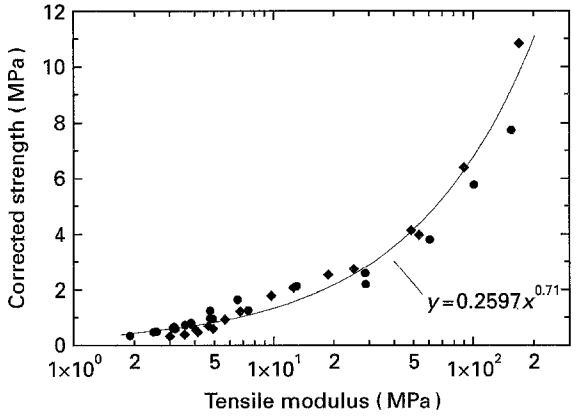

Figure 19 Relationship between the correlated strength ($\sigma_m(1 + \varepsilon_m)T_r/T$, see text for explanation) and the uniaxial tensile modulus from uniaxial constant strain rate tests on (●) HTPB/AP and (◆) GAP/PSAN propellant over three decades of constant strain rate. The combined data have been fitted to a power law.

Fig. 17a and b for GAP/PSAN. Shown are values of G' along with $E_T/3$ over a range of temperatures at two different constant strain rates, 0.009 67 and 0.0967 s^{-1}. Similar results were observed for HTPB/AP at constant strain rates of 0.009 67 and 0.0967 s^{-1} (Fig. 18a and b).

The authors have noted a relationship between strength, σ_m, and the tensile modulus, E_T, obtained from uniaxial constant strain rate tests on both HTPB/AP and GAP/PSAN propellant over a range of constant strain rates. There is no theoretical reason why this functional relationship should exist; however, it has been observed by others working with filled polymer solid propellants [17]. When the strength is defined in terms of strain and temperature-corrected strength ($\sigma_m(1 + \varepsilon_m)T_r/T$), where ε_m is the strain at maximum strength, T_r is a reference temperature and T is the test temperature at which the strength and the tensile modulus were measured, the corrected strength versus E_T for both the filled HTPB/AP and GAP/PSAN solid propellants can be described by a single power law relationship (Fig. 19). This suggests the potential for relating G' to σ_m through E_T.

5. Conclusions

These findings represent an important step forward in the use of dynamic mechanical analyses to aid in the complete characterization of filled polymer solid propellants. The results demonstrate that it is possible to compare $3G'$ measured at different dynamic strains and frequencies with the incremental tangent moduli obtained at corresponding uniaxial strains from constant strain rate tests on specimens with a JANNAF geometry. The comparisons are most favourable when the concave-up region of the stress–strain curve extends only up to approximately 2.0% strain. It was observed that G' obtained at a dynamic shear strain of 2.0% provided the best overall correlation with $E_T/3$ measured over a range of temperatures and strain rates.

Acknowledgements

The authors thank M. Kervarec for the preparation of the uniaxial test specimens and his technical assistance with the laboratory equipment, and D. Gilbert for the preparation of the dynamic shear test specimens. We also thank Mr F. Wong for the useful discussions regarding the work.

References

1. R. G. STACER, C. HÜBNER and D. M. HUSBAND, *Rubber Chem. Technol.* **63** (1990) 488.
2. R. G. STACER and D. M. HUSBAND, *Rheol. Acta* **29** (1990) 152.
3. D. A. TOD, in "Technology of Energetic Materials: Manufacturing and Processing Valuation of Product Properties", 18th International Conference of ICT, Karlsruhe, FRG, July 1987, edited by Herausgeber (Fraunhofer-Institut für Chemische Technologie, 1987) p. 44-1.
4. D. M. HUSBAND, D. C. FERGUSON and F. Q. ROBERTO, *CPIA Pub.* **435** (1985) 135.
5. R. G. STACER and D. M. HUSBAND, *Propellants Explos. Pyrotech.* **16** (1991) 167.
6. K. J. MIN and F. N. KELLY in "Technology of Polymer Compounds and Energetic Materials", 21st International Conference of ICT, Karlsruhe, FRG edited by Herausgeber (Fraunhofer-Institut für Chemische Technologie, 1990) p. 28-1.
7. D. M. HUSBAND, *Propellants Explos. Pyrotech.* **17** (1992) 196.
8. M. BAUMGAERTEL and H. H. WINTER, *Rheol. Acta* **28** (1989) 511.

9. N. ORBEY and J. M. DEALY, *J. Rheol.* **35** (1991) 1035.
10. R. FULCHIRON, V. VERNEY, P. CASSAGNAU, A. MICHEL, P. LEVOIR and J. AUBART, *ibid.* **37** (1993) 17.
11. M. SIMHAMBHATLA and A. I. LEONOV, *Rheol. Acta* **32** (1993) 589.
12. J. D. FERRY, "Viscoelastic Properties of Polymers", 3rd Edn (Wiley, New York, 1980).
13. I. M. WARD, "Mechanical Properties of Solid Polymers", 2nd Edn (Wiley, New York, 1979).
14. W. N. FINDLEY, J. S. LAI and K. ONARAN, "Creep and Relaxation of Nonlinear Viscoelastic Materials", 1st Edn (Dover, New York, 1989).
15. "Uniaxial Tensile Tests at Constant Strain Rate", Suplement to "JANNAF Solid Propellant Mechanical Behaviour Manual", (John Hopkins University Applied Physics Laboratory, Silver Spring, MD, 1970) Chemical Propulsion Information Agency Publication 21.
16. E. J. S. DUNCAN, *J. Appl. Polym. Sci.* **56** (1995) 365.
17. D. L. MARTIN, Jr, Chemical Propulsion Information Agency Publication **490** (The John Hopkins University Applied Physics Laboratory, Silver Spring, MD, June 1988).

Received 12 January
and accepted 8 September 1995